Pharm Res (2012) 29:559–573
DOI 10.1007/s11095-011-0592-5

RESEARCH PAPER

Polyamide Nanocapsules and Nano-emulsions Containing Parsol® MCX and Parsol® 1789: *In Vitro* Release, *Ex Vivo* Skin Penetration and Photo-Stability Studies

Ibrahim Hanno • Cecilia Anselmi • Kawthar Bouchemal

Received: 19 April 2011 / Accepted: 13 September 2011 / Published online: 23 September 2011

ABSTRACT

Purpose To prepare polyamide nanocapsules for skin photo-protection, encapsulating α-tocopherol, Parsol®MCX (ethylhexyl methoxycinnamate) and/or Parsol®1789 (butyl methoxydibenzoylmethane).

Methods Nanocapsules were obtained by combining spontaneous emulsification and interfacial polycondensation reaction between sebacoyl chloride and diethylenetriamine. Nano-emulsions used as control were obtained by the same process without monomers. The influence of carrier on release rate was studied *in vitro* with a membrane-free model. Epidermal penetration of encapsulated sunscreens was *ex vivo* evaluated using Franz diffusion cells. Ability of encapsulated sunscreens to improve photo-stability was verified by comparing percentage of degradation after UV radiation exposure.

Results Sunscreen-containing nanocapsules (260–400 nm) were successfully prepared; yield of encapsulation was >98%. Parsol®MCX and Parsol®1789 encapsulation led to decreased release rate by up to 60% in comparison with nano-emulsion and allowed minimum penetration through pig ear epidermis. Presence of polyamide shell protected encapsulated sunscreen filters from photo-degradation without affecting their activity.

Conclusions Encapsulation of Parsol®MCX and Parsol®1789 into oil-core of polyamide nanocapsules allowed protection from photo-degradation, controlled release from nanocapsules, and limited penetration through pig ear epidermis.

KEY WORDS photo-stability · polyamide nanocapsules · skin penetration · sunscreens

INTRODUCTION

Sun protection is one of the most fundamental requires for our skin, the skin is subject to the action of sunlight daily, the exaggerating exposure of sun ultraviolet (UV) rays UVA and UVB have many harmful effects on our skin, such as rashes, skin lesions, photosensitivity, photo-allergy, skin aging, hyperkeratosis and hypertrichosis (1–3).

Parsol® MCX and Parsol® 1789, chemically known as ethylhexyl methoxycinnamate and butyl methoxydibenzoylmethane respectively, are the most common sunscreen agents used in a variety of consumer products for their capacity to absorb and dissipate UV radiations (3, 4). By absorbing UV rays, Parsol® MCX and Parsol® 1789 also help to prevent the integrity of other cosmetic ingredients from photo-degradation, to stabilize complex formulations and color cosmetics. Consequently, Parsol® MCX and Parsol® 1789 are widely used in a variety of personal care products like nail polish, sunscreen lotions, creams, lipcares, shampoos and fragrances.

However, successful development of Parsol® MCX and Parsol® 1789 formulations encounters two major challenges.

I. Hanno · K. Bouchemal (✉)
Faculty of Pharmacy University of Paris-Sud 11 UMR CNRS 8612
5 Rue J.B. Clément
92296 Châtenay-Malabry cedex, France
e-mail: kawthar.bouchemal@u-psud.fr

I. Hanno · C. Anselmi
Faculty of Pharmacy
Interdepartmental Centre of Cosmetic Science & Technology
University of Siena
Via della Diana, 2
53100 Siena, Italy

K. Bouchemal
Physicochimie Pharmacotechnie & Biopharmacie
Faculté de pharmacie
5 Rue J.B. Clément
92296 Châtenay-Malabry, France

Firstly, despite their sun protective abilities, Parsol® MCX and Parsol® 1789 could penetrate the skin and to cause photosensitivity. They have also been linked to contact eczema and are believed to be a contributing factor in the recent rise of melanoma cases with sunscreen users. Being totally derivatives from chemical molecules, their direct contact with the skin is not very desired (5). Secondly, from a physico-chemical point of view, the oily nature of Parsol® MCX and the poor water solubility of Parsol® 1789 represent serious concerns for their formulation.

Ideally, a formulation should *(i)* solubilize Parsol® 1789 and be adapted to the oily nature of Parsol® MCX *(ii)* protect them from sun degradation, *(iii)* control sunscreen release and *(iv)* have limited penetration through the skin. The strategy proposed to reach these objectives consists on the encapsulation of Parsol® MCX and Parsol® 1789 in oil-containing nanocapsules (NCs). Despite all these presumed advantages of Parsol® encapsulation, few research works were oriented towards this strategy (6–8).

Because Parsol® MCX and Parsol® 1789 protect the skin from harmful UVA (320–400 nm) and UVB (290–320 nm) rays respectively, the combination of these two sunscreen agents in the same formulation is particularly interesting for efficient skin photo-protection. It is worth to note that no research work has reported the association of the two Parsols MCX and 1789 in the same NC formulation.

In the work presented here, Parsol® MCX and Parsol® 1789 will be encapsulated into oil-containing NCs obtained by spontaneous emulsification and interfacial polycondensation method (9–13). Parsol® MCX, Parsol® 1789 will be encapsulated alone or mixed together or in combination with α-tocopherol. It has been demonstrated that this antioxidant agent largely used as supplement for cosmetics to reduce radiation-induced skin damage (14–16) was able to increase photo-protection provided by sunscreens and to improve their own photo-stability (17). The results will be compared to nano-emulsion (NE) prepared in the same conditions that NCs but without monomers. *In vitro* release and *ex vivo* skin penetration of Parsol® MCX and Parsol® 1789 contained into NCs will be then evaluated. Finally, the possibility of NCs to increase the Parsol® photo-stability will be explored.

MATERIALS AND METHODS

Materials

Monomers (sebacoyl chloride (SC) and diethylenetriamine (DETA)), solvents (ethanol (96% *v/v*) acetone and isopropanol) and α-tocopherol were supplied from Sigma—Aldrich, France. Chloroform-d (99.8% D) from Carlo Erba Reactifs-SDS, France. Surfactants (Tween® 80 "Polysorbate 80", Span® 80 "Sorbitan monooleate" and Montanov® 68 "Cetearyl Alcohol, Cetearyl Glucoside") were supplied from Seppic, France. Amphisol® K "Potassium Cetyl Phosphate" was obtained from Res Phrama, Italy. Sunscreen filters (Parsol® MCX "ethyhexyl methoxycinnamate" and Parsol® 1798 "butyl methoxydibenzoylmethane") were obtained from DSM Nutritional Products, Germany. Finsolv® TN "C_{12}–C_{15} alkyl benzoate" was obtained from Innospec Active Chemicals, Italy. Fenossiparaben as preservative composed of phenoxyethanol, methylparaben, butylparaben, ethylparaben and propylparaben, was obtained from Sinerga, Italy. (Kathon™ CG "methyl chloro isothiazolinone and methyl isothiazolinone") were supplied from Dow Italia s.r.l, Milan, Italy.

Preparation and Characterization of Polyamide Film

Polyamide film obtained by interfacial polycondensation reaction was first achieved in the aim to observe the reaction at the macroscopic scale and to characterize the polymer formed. The manufacturing process of polyamide film by interfacial polycondensation reaction was achieved according to the method developed by Bouchemal *et al.* (10). The organic phase was composed of 200 mL cyclohexane and 10^{-2} mol (1.20 g) of lipophilic monomer (sebacoyl chloride). The aqueous phase was composed of 10^{-1} mol of DETA (5.16 g) in 400 mL water contained in a 1-liter beaker. The SC/DETA molar monomers ratio was 1/10. The beaker was closed to limit the cyclohexane evaporation. The experiment was stopped after 7 days. At the end of the experiment, the polymer was washed with distilled water and freeze-dried (Christ Alpha 1–4 freeze-dryer. Bioblock Scientific, Illkirch, France) and stored at +4°C until use.

The polyamide film was then characterized by using Attenuated total reflectance-Fourier transform infra red (ATR-FTIR) spectroscopy and high-resolution solid-state ^{13}C-NMR. Polyamide film Infrared spectrum was obtained with an attenuated total reflectance infrared (ATR-IR) spectrometer (FT/IR-4100, JASCO) operating at 4 cm^{-1} resolution. Fifty scans were accumulated in each run and referred to air. The ATR sampling device utilized a diamond internal reflection element embedded into a ZnSe support/focusing element in a single reflection configuration. The resultant spectrum over the range of 4000–650 cm^{-1} was analyzed using the IR Protein Secondary Structure Analysis program (JASCO Co).

High-resolution solid-state ^{13}C-NMR spectrum of the polyamide film was obtained at 10 kHz (Bruker-500 MHz spectrometer, Bruker Instrument Inc. Wissembourg, France). The conventional cross polarization and magic angle spinning with ^{1}H high-power dipolar decoupling technique was used.

Preparation of the Oil Phases for NE and NC Formulations

Different oil compositions were used for NE and NC formulations:

- P1 was composed of Parsol® MCX in the form of oil.
- P2 was composed of Parsol® 1789 in the form of powder dissolved in Finsolv® TN. Noteworthy; Finsolv® TN is the unique non-toxic, non-irritating, non-sensitizing, non-comedogenic and practically odorless emollient ester. The solubility limit of Parsol® 1789 in Finsolv® TN (14% *w/w*) was experimentally determined by the progressive dissolution of Parsol® 1789 in 1000 mg of Finsolv® TN under magnetic stirring at 20°C.
- P3 was composed of a mix of Parsol® 1789 and Parsol® MCX. Parsol® 1789 was dissolved in Parsol® MCX. Solubility limit of Parsol® 1789 into Parsol® MCX (25% *w/w*) was experimentally determined by the progressive dissolution of Parsol® 1789 in 1000 mg of Parsol® MCX under magnetic stirring at 20°C.
- P4 was composed of a mix of the phase P1 and α-tocopherol (Parsol® MCX/α-tocopherol) (91/9% *w/w*).
- P5 was composed of a mix of the phase P2 and α-tocopherol (Parsol® 1789/Finsolv® TN/α-tocopherol) (13/78/9% *w/w*).
- P6 was an oil phase exclusively composed of α-tocopherol as control.

NE and NC Preparation

NEs were prepared according to the method described by Bouchemal and co-workers (18). Briefly, 200 mg of oil phase (P1, P2, P3, P4, P5 or P6) prepared according to the previous section, and the lipophilic surfactant Span® 80 (43 mg) were dissolved in 20 mL of acetone as water-miscible solvent. This organic phase was then poured by using a 20 mL syringe under moderate magnetic stirring into an aqueous phase composed of the hydrophilic surfactant Tween® 80 (68 mg) dissolved in 40 mL of water. The o/w emulsion was formed instantaneously by the acetone-water interdiffusion leading to the formation of nano-droplets.

Polyamide NCs were prepared according to the same method used for NE preparation by adding a lipophilic monomer SC (119.57 mg) to the organic phase and hydrophilic monomer DETA (515.85 mg) to the aqueous phase (10, 12). When the organic phase was poured into the aqueous phase by using a 20 mL syringe, the two monomers reacted at the interface between oil and acetone/water mixture, forming a polyamide membrane around the oil droplets leading to the formation of NCs. The effect of oil content on NE and NC formation was optimized by progressively increasing the oil weighted in the organic phase from 200 to 1000 mg.

Whatever the formulation (NEs or NCs), the magnetic stirring was maintained during 30 min. Then the totality of the solvent and a part of the water were removed by evaporation during 30 min at 40°C under reduced pressure (97 mbar). The final volume was adjusted to 20 mL. The purification of NC suspensions was achieved by dialysis using a Spectra/Por membrane with a molecular weight cut-off of 100,000 g/mol (Biovalley, Marne la Vallée, France) twice for 1 h, and twice for 12 h against 1 L of distilled water.

To evaluate the efficacy of the dialysis step to eliminate unreacted DETA, ^{1}H-NMR spectroscopy (300 MHz—Bruker MSL-400 spectrometer, Bruker Instrument Inc. Wissembourg, France) was used to analyze the dispersing media of NC suspension after evaporation and dialysis steps.

The dispersing medium was isolated from NC suspension by ultracentrifugation (Optima™ LE-80 K Ultracentrifuge, BEKMAN-COULTER Instruments, USA). Ultracentrifugation of 4.5 g of each NC suspension was carried out in Beckman Optima™ tubes (11 mL) housed in a 70.1 TI rotor in an Optima™ MAX Tabletop ultracentrifuge. All tubes were centrifuged at 40,000 rpm for 30 min at 20°C. Each dispersing medium was then completely evaporated at 40°C under reduced pressure (97 mbar) and re-suspended into $CDCl_3$.

Preparation of Emulsions

The ingredients of the emulsions were summarized in Table I. The oil soluble ingredients (Montanov® 68, Finsolv® TN, Parsol® MCX and/or Parsol® 1798) were weighted in a metallic beaker. This oil phase was heated to a temperature of 70°C under mechanical stirring.

Aqueous phase was prepared by adding water to Amphisol® K contained in a metallic beaker. This phase was then heated to 70°C under mechanical stirring. The oil and the aqueous phases were emulsified by pouring the oil in the aqueous phase at a temperature of 70°C under intense agitation by the turboemulsifier (Silverson LHR mod. SL 2) for 1 min.

The resulting emulsion was then poured in a water bath accompanied with a slow stirring by a planetary stirrer. Reached room temperature, thermolabile ingredients (lipophilic Fenossiparaben and hydrophilic Kathon™ CG) were incorporated. Then a final turbo shot was achieved for about 4 min.

Size Measurements of NEs and NCs

The hydrodynamic diameter of NEs and NCs and the size distributions were determined at 25°C by quasi-elastic light scattering using a Nanosizer® N4 PLUS (Beckman-Coulter, Villepinte, France). The scattered angle was fixed

Table I Ingredients for the Formulation of Emulsions with Sunscreen Filters

Ingredients	Parsol® MCX free EM(%) *w/w*	Parsol® 1789 free EM (%) *w/w*	Parsol® 1789 + Parsol® MCX free EM %) *w/w*
Montanov® 68 Cetearyl Alcohol, Cetearyl Glucoside	5.00	5.00	5.00
Finsolv® TN C_{12}-C_{15} Alkyl Benzoate	18.00	18.86	17.67
Parsol® MCX Ethyhexyl Methoxycinnamate	1.00	–	1.00
Parsol® 1789 Butyl Methoxydibenzoylmethane	–	0.14	0.33
Fenossiparaben Phenoxyethanol, Methylparaben, Butylparaben, Ethylparaben, Propylparaben	1.00	1.00	1.00
Water	74.45	74.45	74.45
Amphisol® K Potassium Cetyl Phosphate	0.50	0.50	0.50
Kathon™ CG Methyl Chloro Isothiazolinone, Methyl Isothiazolinone	0.05	0.05	0.05

at 90° and 60 µL of each sample was diluted in 2 mL of MilliQ® water.

Scanning Electron Microscopy Observations

NC morphology was analyzed by Scanning Electron Microscopy (SEM) using a LEO 1530 (LEO Electron Microscopy Inc., Thronwood, NY) operating at 3 kV with a filament current of about 0.5 mA (CNRS CECM, Vitry-sur-Seine, France). Noteworthy, SEM microphotographs were obtained only for NCs because NEs were deformed by the drying and the SEM observation conditions.

Transmission Electron Microscopy (TEM)

TEM observations were assessed using a Phillips EM 208 apparatus operating at 80 kV (UMR CNRS 8080, Orsay, France). NC suspensions or NEs were directly laid on a carbon grid and stained with phosphotungstic acid 1% (pH 7.4) before observation.

Yield of Encapsulation

The yields of sunscreen agent encapsulation (Y) was calculated according to equation Eq. 1 (19, 20):

$$Y = \frac{L}{T}100 = \frac{T - F}{T}100 \quad (1)$$

where Y is the yield of sunscreen agent encapsulation, L is the concentration of sunscreen agent loaded in the NCs (µg/mL), F is the concentration of sunscreen agent found in the dispersing medium after separation of the NCs (µg/mL), and T is the concentration of sunscreen agent recovered from the total NC suspension (µg/mL).

To be comparable, all concentrations were reported to the same volume for each sample. Free unloaded sunscreen agent contained in the dispersing medium was isolated from sunscreen agent-loaded NC suspension by ultracentrifugation (Optima™ LE-80 K Ultracentrifuge, BEKMAN-COULTER Instruments, USA). Ultracentrifugation of 4.5 g of each NC suspension was carried out in Beckman Optima™ tubes (11 mL) housed in a 70.1 TI rotor in an Optima™ MAX Tabletop ultracentrifuge. All tubes were centrifuged at 40,000 rpm for 30 min at 20°C. NCs were isolated and completed to 4.5 g using (Water/Tween® 80) mixture at 0.33% *v/v*. This washing operation was reproduced three times. The same protocol was used to determine the yield of NE formation corresponding to the percentage of oil converted into NE.

Determination of Parsol® MCX and Parsol® 1789 Concentrations

The concentration of sunscreen agent associated with the NCs and the total sunscreen agent concentration recovered in the NC suspension were obtained after their solubilization following the protocol described by previous works (18). Typically, 10 mL of Isopropanol were added to NC suspension. The NCs were allowed to dissolve 30 min on ultrasounds. The amount of sunscreen filter loaded in NCs was determined by UV–VIS Scanning Spectrophotometer (UV-2101PC, SHIMADZU, France), the absorbance was measured at 308 nm in the case of Parsol® MCX and 358 nm in the case of Parsol® 1789. A solution of pure Isopropanol served as a reference. Experiments were performed in triplicate.

The equations of the calibration curves were $y = 94.26133x + 0.04505$, $r^2 = 0.9996$, and $y = 99.55133x + 0.09955$, $r^2 = 0.9990$, for Parsol® MCX and Parsol® 1789, respectively.

In Vitro Release Experiments

This study was performed with the membrane-free model for NE and NC preparations according to Wissing and coworkers (21). This method allows the investigation of sunscreen release without using membranes. Here, the diffusion of the sunscreen agent from the formulation to a lipophilic acceptor medium is observed.

One milliliter of each NE or NC preparation was placed in a glass tube. Four milliliters of an aqueous 3% *w/w* Polysorbate 80 solution (PH 5.54) were added. Then, 10 mL of lipophilic medium composed of Finsolv® TN were carefully placed on the top of the aqueous NE or NC preparations. Finsolv® TN served as acceptor medium because both studied sunscreens are well soluble in this medium. The samples were stored at 32°C in a temperature-controlled shaking chamber at 100 rpm.

After scheduled incubation times (5 min, 1 h, 2 h, 4 h, 6 h, 18 h and 24 h), one milliliter of each sample were taken out of the oily phase and immediately replaced with one milliliter of lipophilic medium. Each sample was diluted with 9 mL of ethanol (96% *v/v*) and analyzed by UV–VIS Scanning Spectrophotometer (UV-2101PC, SHIMADZU, France). The absorbance was measured at 308 nm in case of Parsol® MCX and 358 nm in case of Parsol® 1789. A solution of Finsolv® TN/ethanol (1:9) (*v/v*) served as reference.

Each NE and NC preparation was applied and analyzed in triplicate.

NC and NE *Ex Vivo* Skin Penetration

Animals

The ethical and practical problems of using human tissues have led to the development of a variety of model systems including *ex vivo* animal tissues. Among the larger experimental animals, the pig has the advantage of being remarkably similar to human in terms of anatomy, physiology, metabolism, and histology. Furthermore, previous research works have reported the excellent correlation between human and porcine skin (22). Pig skin was found to have a closer permeability character than rat skin to human skin, particularly for lipophilic penetrants.

Experiments were carried out on female pigs weighing between 60 and 63 kg in average. All experiments on animals adhered to the Communities Commission Directive (DE/86/609/CEE) and were performed in conformance with the French Ministry of Agriculture Permission No. 78–16.

Pigs were sacrificed by intravenous injection (20 mL) of overdosed sodium phenobarbital (Dolethal, Vetoquinol Laboratory, Lure, France). Pig ears were then excised with a scalpel and cleaned from hairs and stored frozen for further uses.

Skin Membrane Preparation

One hour before its use, pig ears were taken out from the freezer to be thawed. Then, epidermal membranes were obtained by soaking the whole skin in water for 120 s at 60°C, after which the epidermis was carefully separated from the dermis with tweezers, washed with water, dried with soft paper and immediately used for the experiments (21, 23, 24). Previous research works demonstrated the maintenance of stratum corneum barrier characteristics after storage in the reported conditions (25).

Ex Vivo Skin Penetration Experiments

This study was carried out with vertical Franz glass diffusion cells. These cells consist of donor and receptor chambers between which the epidermal membrane is positioned. The area for diffusion was 3.24 cm^2 and the receptor chamber

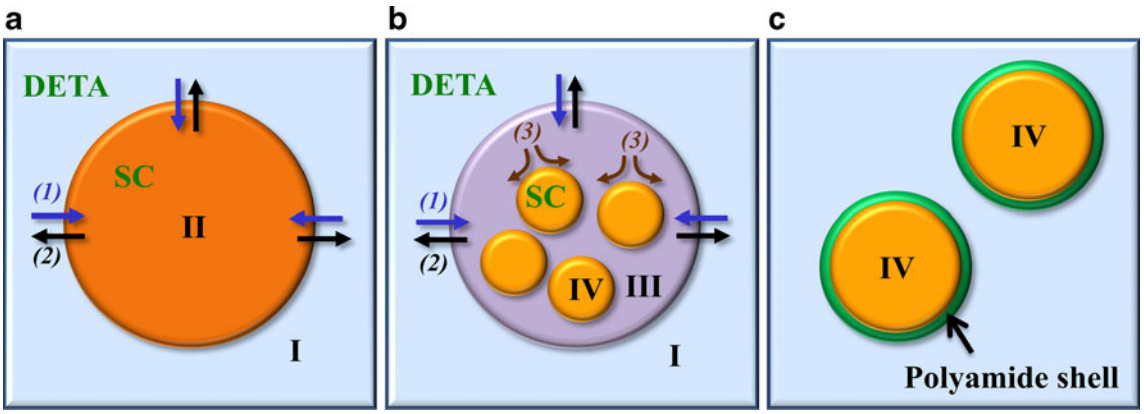

Fig. 1 (**a**) initial state when water phase (larger sphere (**I**)) is mixed with organic phase composed of oil, acetone and SC (internal sphere (**II**)). (**b**) A supersaturation layer appears (**III**) resulting from water-acetone interdiffusion and oil nucleation (**IV**). (**c**) Final state represents the growth of oil droplets and the interfacial polycondensation between SC and DETA. (***1***) diffusion of water into organic phase, (**2**) diffusion of acetone in water, and (**3**) oil nucleation.

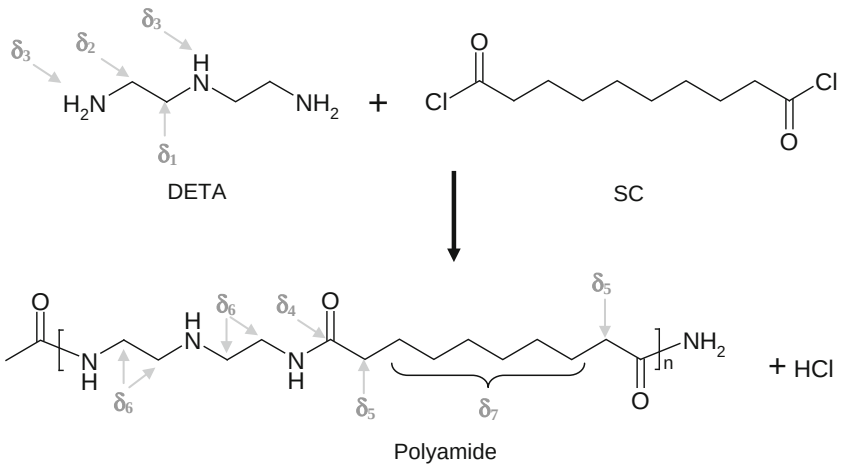

Fig. 2 Synthetic scheme of chemical reaction of polyamide film formation between diethylenetriamine (DETA) and sebacoyl chloride (SC). The chemical shifts for DETA in and polyamide film were obtained in the liquid state in $CDCl_3$ at 300 MHz were $\delta_1 = 2.6$, $\delta_2 = 2.48$ and $\delta_3 = 1.02$ ppm. The polyamide high-resolution ^{13}C-NMR spectrum of the polyamide film in the solid-state allowed the identification of the chemical shifts: $\delta_4 = 172$, $\delta_5 = 44$, $\delta_6 = 35$ and $\delta_7 = 28$ ppm.

volume was 13 mL. The receptor chamber was maintained at 37°C in order to ensure the temperature of 32°C on the surface of the membrane. The receptor medium consisted of a solution of Finsolv® TN/ethanol (1/9) (v/v). The composition of the receptor medium was chosen because of the insufficient solubility of the studied sunscreens in aqueous

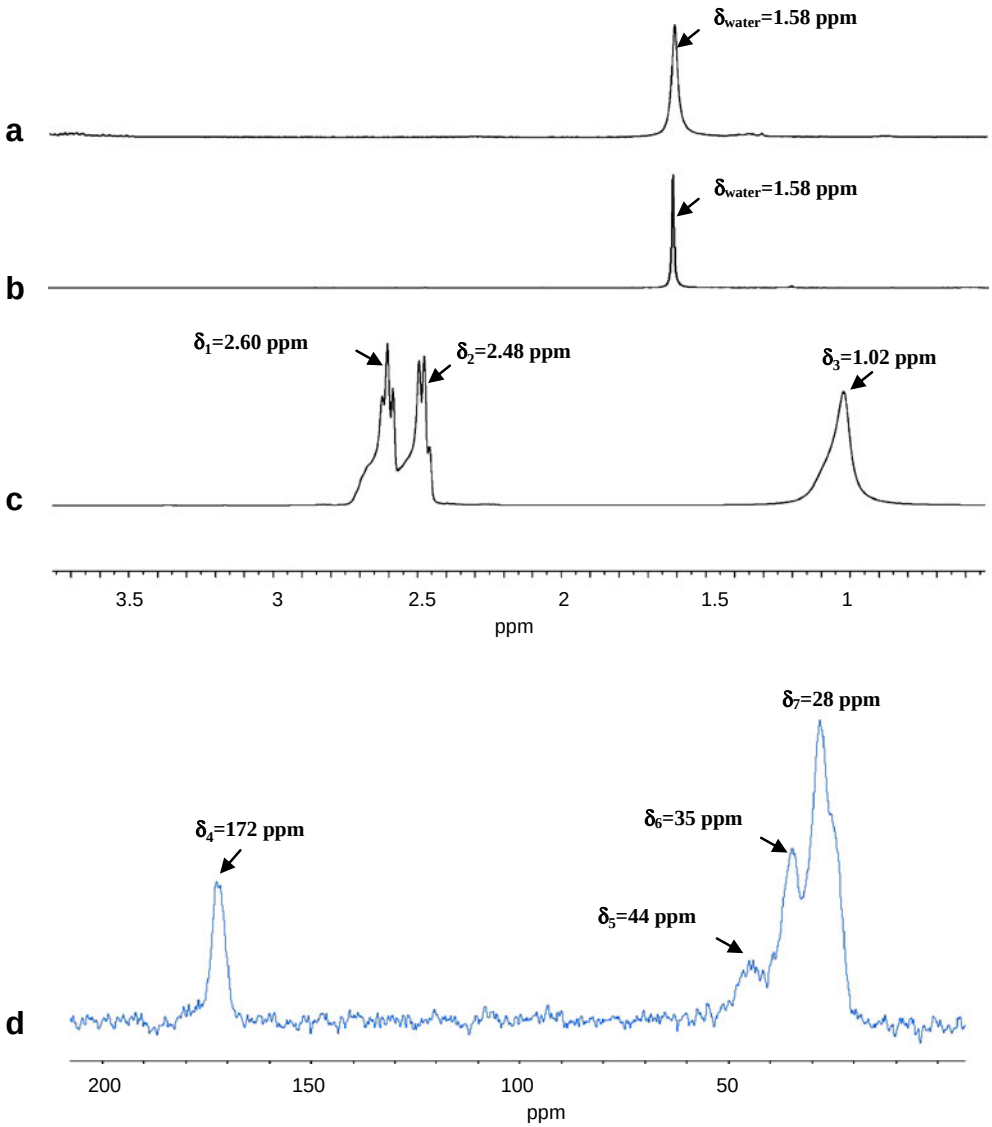

Fig. 3 Typical ^{1}H-NMR spectrum of the NC supernatant before (**a**) and after (**b**) dialysis compared to the spectrum of DETA presented in (**c**). The spectra A, B and C were obtained in the liquid state in $CDCl_3$ at 300 MHz. The high-resolution ^{13}C-NMR spectrum of the polyamide film in the solid-state is presented in (**d**).

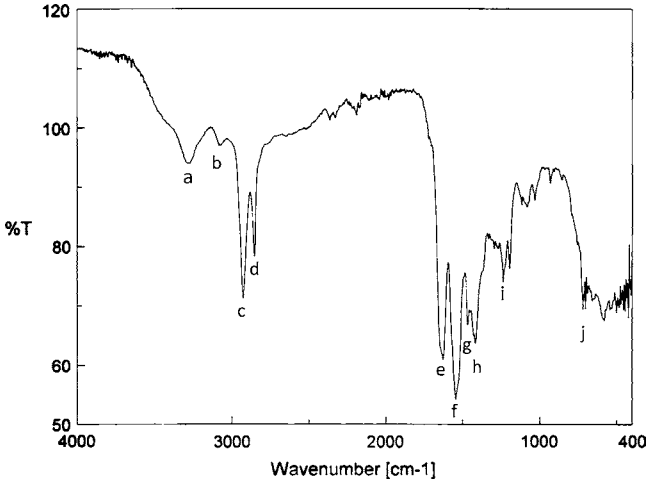

Fig. 4 ATR-IR spectrum of polyamide film obtained by the interfacial polycondensation of diethylenetriamine (DETA) and sebacoyl chloride (SC).

media. Both studied sunscreens are well soluble in the chosen receptor medium.

Each cell contained a magnetic bar and was stirred during the experiment at 500 rpm. Then, 200 µL of each NE and NC preparation were evenly spread on the surface of the skin and 100 µL samples were taken out from each receptor chamber and immediately replaced with 100 µL fresh receptor medium. Samples were taken out after 5 min, 1 h, 2 h, 4 h, 6 h, 18 h and 24 h and diluted with 900 µL Finsolv® TN/ethanol 96% (1/9) (*v*/*v*). Samples were analyzed by UV–VIS Scanning Spectrophotometer (UV-2101PC, SHIMADZU, France). A solution of Finsolv® TN/ethanol (1/9) (*v*/*v*) served as reference.

Each NE and NC preparation was applied and analyzed in triplicate.

Activity and Photo-stability Studies

Activity of encapsulated sunscreens was verified according to the European Cosmetic Toiletry and Perfumery Association (COLIPA) SPF *in vitro* test (26) by comparing SPF "Sun Protection Factor" values of NC preparations with emulsions containing the same proportion of free sunscreens by using (Labsphere—UV—1000S Ultraviolet Transmittance Analyzer).

A surgical patch of TRANSPORE TM (3 M company) with area of 15 cm^2, was used as substrate for this experiment (27). Typically, 2 mg/cm^2 of each tested preparation were distributed on the substrate surface with the tip of a Pasteur

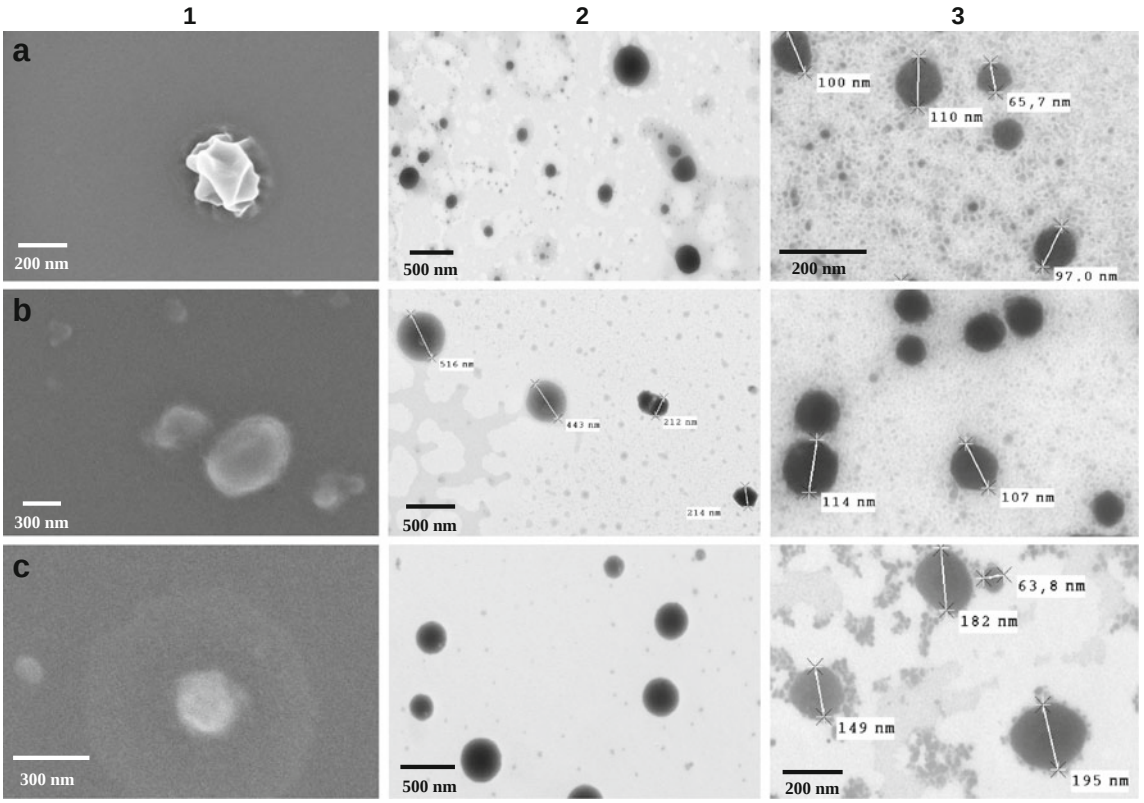

Fig. 5 SEM (1) and TEM observations of the NCs (2) and NEs (3). Oil phase was composed of Parsol® 1789 (**a**), Parsol® MCX (**b**), and Parsol® 1789/ Parsol® MCX (**c**).

pipette, the stratification of the sample was done manually, using a latex glove (Global), taking care to distribute the product with three longitudinal movement back and forth, fifteen circular motion and, again, three longitudinal motions in a no longer than 30 s. For each preparation tested were performed 5 independent samples, determining the SPF of 12 different points of each sample. The instrumental determination was performed after 15 min, according to the standard operations of cosmetics containing aqueous phases (26).

The ability of encapsulated sunscreens to improve photostability was verified according to the COLIPA *in vitro* test (28) by comparing the percentage of degradation of NC preparations with free sunscreens contained in the NEs and the emulsions. NE and emulsion were used as a reference for this study to bring up the role of polyamide membrane to protect the encapsulated sunscreen filters. The photostability was determined after UV radiation exposure for 5, 10 and 20 MED "Minimal Erythema Dose", correspondent to 0.15, 0.3 and 0.6 J/cm^2, by using an optical bench L.O.T. ORIEL ITALIA (model 70234), equipped with a Xenon lamp (Universal Arc Lamp Housing, model 66000) calibrated by a radiometer probe Goldlux UVA and UVB.

The power of the lamp in μW/cm^2 was measured 10 min after the lamp powered on, by placing the detector at 40 cm from the glass of the lamp itself. The absolute power is determined in both UVB and UVA range (from 280 to 400 nm). Then, the calibration line was calculated in two different ranges: from 1 to 4 J/cm^2 and from 100 to 400 mJ/cm^2.

About 10 mg of each tested preparation were deposited on a thin-layer vial with an optical path of 0.01 mm (Hellma). After irradiation exposure, the irradiated sample was recovered from the vial with Isopropanol, reported to 10 mL of final volume and analyzed by UV–VIS scanning spectrophotometer to calculate the percentage of degradation.

RESULTS & DISCUSSION

Oil containing polyamide NCs were used in the present work to encapsulate Parsol® MCX and Parsol® 1789 in the presence of α-tocopherol as anti-oxidant agent. The oil core of NCs was perfectly adapted as a carrier for these sunscreen filters. It is expected that polyamide shell protects sunscreen agents from photo-degradation and to control sunscreen release. Furthermore, due to the photo-sensibility provoked by the skin penetration of Parsols, ideally, their encapsulation should limit their penetration through the skin. The encapsulation of Parsol® MCX and Parsol® 1789 in polyamide NCs was obtained by the spontaneous emulsification combined to interfacial polycondensation method (9–12). We propose to schematise the spontaneous emulsification combined to interfacial polycondensation process by three states. We represent the initial state as a sphere corresponding to the organic phase and a cube corresponding to aqueous phase as shown in Fig. 1a. When the organic phase composed of oil/acetone is mixed with the aqueous phase, a supersaturation layer appears resulting from water-acetone interdiffusion. The oil becomes greatly supersaturated; the solubility of oil molecules falls so considerably that they precipitate by nucleation (Fig. 1b). Final state represents the growth of oil droplets (Fig. 1c) and the interfacial polycondensation between DETA and SC (Fig. 2).

Table II ATR FT-IR Band Assignments of Polyamide Film Obtained by the Interfacial Polycondensation of Diethylenetriamine (DETA) and Sebacoyl Chloride (SC)

Code	Band (cm^{-1})	Assignment
a	3283	Free N–H stretching N-H stretching
b	3079	Hydrogen bonded N-H stretching
c	2924	Asymmetric CH_2 stretch
d	2851	Symmetric CH_2 stretch
e	1623	Amide I
f	1540	Amide II
g-h	1400–1470	CH_2 deformation
i	1122, 1079	C-NH_2 in primary aliphatic amines
j	920–970	CO-NH in plane vibration

At the end of the polymerization of DETA and SC, the acetone was evaporated under reduced pressure. To avoid any toxic effect of acetone and DETA, the performance of the evaporation to remove acetone and the dialysis step to eliminate DETA were verified. The dispersing media of NC suspensions were analyzed after evaporation and dialysis steps by ^{1}H-NMR spectroscopy. The ^{1}H-NMR spectra presented in Fig. 3a, b were characterized by the disappearance of the bands characteristic of acetone at 2.16 ppm and DETA usually present at $\delta_1 = 2.6$, $\delta_2 = 2.48$ and $\delta_3 = 1.02$ ppm (Fig. 3c).

Table III Optimization of Oil Content. Mean Hydrodynamic Size Measurements of the NCs Prepared with α-tocopherol by Small-angle Light Scattering

Quantity of α-tocopherol (mg) for 20 mL of acetone	Small population (nm)	Large population (nm)	Volume fraction of the large-size population (%)
200	270 ± 20	None	0
400	298 ± 97	None	0
600	437 ± 71	4636 ± 247[a]	20
800	[b]	[b]	[b]
1000	[b]	[b]	[b]

[a] Presence of small quantity of oil at the surface

[b] Partial phase separation, presence of oil at the surface

Table IV Small-Angle Light Scattering Size Measurements of NE and NC Formulations Prepared with Different Sunscreen Agents

Oil phase code	Oil phase composition	NEs		NCs	
		Before evaporation	After evaporation	Before evaporation	After evaporation
P1	PA_1: Parsol® MCX	174 ± 1	169 ± 1	269 ± 55	282 ± 45
P2	PA_2: Parsol® 1789 (14% *w/w*) in Finsolv TN	175 ± 2	174 ± 1	335 ± 55	339 ± 4
P3	PA_1/PA_2 (3:1) (25% *w/w*)	180 ± 8	176 ± 9	392 ± 48	446 ± 23
P4	PA_1/α-toc (10:1)	173 ± 1	174 ± 2	331 ± 18	311 ± 15
P5	PA_2/α-toc (1.4:1)	192 ± 3	187 ± 4	421 ± 13	385 ± 43
P6	α-toc	169 ± 2	167 ± 9	300 ± 18	270 ± 20

ATR-FTIR, ^{1}H-NMR and ^{13}C-NMR Spectra of the Polyamide Film

The process of the spontaneous emulsification combined to interfacial polycondensation is extremely fast, down to the region of milliseconds (10). For this reason, in the aim to characterize the polyamide film obtained when SC interacted with DETA, we used two non-miscible phases composed of SC dissolved in cyclohexane as non-water miscible solvent and DETA dissolved in water. The polyamide film was formed instantaneously when the two phases are in contact. The temperature of the system increases for 1°C. This stage corresponds to the formation of a primary transparent membrane. Within few minutes, the film becomes opaque and the thickness continues growing until reaching equilibrium after few days of reaction. This corresponds to the maximum of polyamide film thickness.

High resolution ^{13}C-NMR spectrum of the polyamide film at the solid state presented in Fig. 3d resulted in sharp and well-resolved peak at $\delta_4 = 172$ ppm which can be easily assigned to amide groups (29). The peaks at $\delta_5 = 44$ ppm and $\delta_6 = 35$ ppm were attributed to the carbons linked to the −C=O and –NH groups respectively. Finally, the central methylene carbons resonated at $\delta_7 = 28$ ppm (30).

ATR-FTIR spectra of the polyamide film presented in Figs. 4 and 5 also confirmed the existence of the amide group function. With the aid of published literature (31–37), the infrared bands were analyzed and assigned in Table II. Infrared absorption at 3283 cm^{-1} (free N–H stretching) (31, 35–37) and the appearance of the band at 3079 cm^{-1} (hydrogen-bonded N–H stretching vibration (31, 35–37) suggesting the presence of hydrogen bonding. This is in agreement with earlier publications (35–37) where, reportedly, there is essentially 100% hydrogen bonding in aliphatic homopolyamides at room temperature. It is interesting that in Fig. 4 we can observe the amide I (corresponding to the end chains of the polymer) and the amide II band at 1623 and 1540 cm^{-1} respectively. Unlike the essentially isolated N-H stretching vibration, the amide I and II modes are more complex vibrations. The amide I mode may be considered to be comprised of contributions from the C=O stretching, the C-N stretching, and the C-C-N deformation vibrations. In polyglycine I, for example, normal coordinate calculations revealed that the potential energy distribution is comprised of 77% C=O stretch, 14% C-N stretch, and 12% C-C-N deformation (38). The amide II band is a mixed mode containing contributions from the N-H in-plane bending, the C-N stretching, and the C-N stretching vibrations.

The bands 2924 and 2851 cm^{-1} were typical for CH_2 asymmetric and symmetric stretching respectively. In Fig. 4, the bands at 1400–1470 cm^{-1} can be clearly attributed to CH_2 deformation bands while 1122 and 1079 cm^{-1} bands

Table V Yield of Encapsulation of Sunscreen Agents into NCs. The Yield of the Production of the NE was 99%

Oil phase code	Oil phase composition	L (μg/mL)	F (μg/mL)	T (μg/mL)	Yield of encapsulation (%) *w/w*
P1	PA_1: Parsol® MCX	9872 ± 28	183 ± 8	10055 ± 18	98.18 ± 0.67
P2	PA_2: Parsol® 1789 (14% *w/w*) in Finsolv TN	1361 ± 14	23 ± 5	1384 ± 10	98.33 ± 0.92
P3	PA_1/PA_2 (3:1) (25% *w/w*)	PA_1: 9853 ± 33	174 ± 11	10027 ± 22	PA_1: 98.27 ± 1.37
		PA_2: 3276 ± 21	34 ± 7	3310 ± 14	PA_2: 98.97 ± 1.21
P4	PA_1/α-toc (10:1)	9865 ± 36	167 ± 13	10032 ± 20	99.34 ± 0.89
P5	PA_2/α-toc (1.4:1)	1373 ± 17	26 ± 6	1399 ± 12	98.14 ± 0.72

L: concentration of sunscreen agent associated with the NC suspension

F: concentration of sunscreen agent found in the dispersing medium after separation of the NC suspension

T: concentration of sunscreen agent recovered from the total NC suspension

can be attributed to C-NH_2 in primary aliphatic amines. Indeed, it has been demonstrated by Bouchemal and co-workers (11) that the polyamide film contains a small amount of DETA. Because the amine diffuses through the polymer to interact with SC in the organic phase. Finally, the infrared absorption at 973 cm^{-1} was characteristic of CO-NH group in plane vibration.

Physico-Chemical Characterization of NE and NC Formulations

Stable NC suspensions without phase separation and without aggregation were obtained only when the concentration of the oil in the organic phase was lower than 2% w/v (400 mg of oil for 20 mL of acetone). For NCs

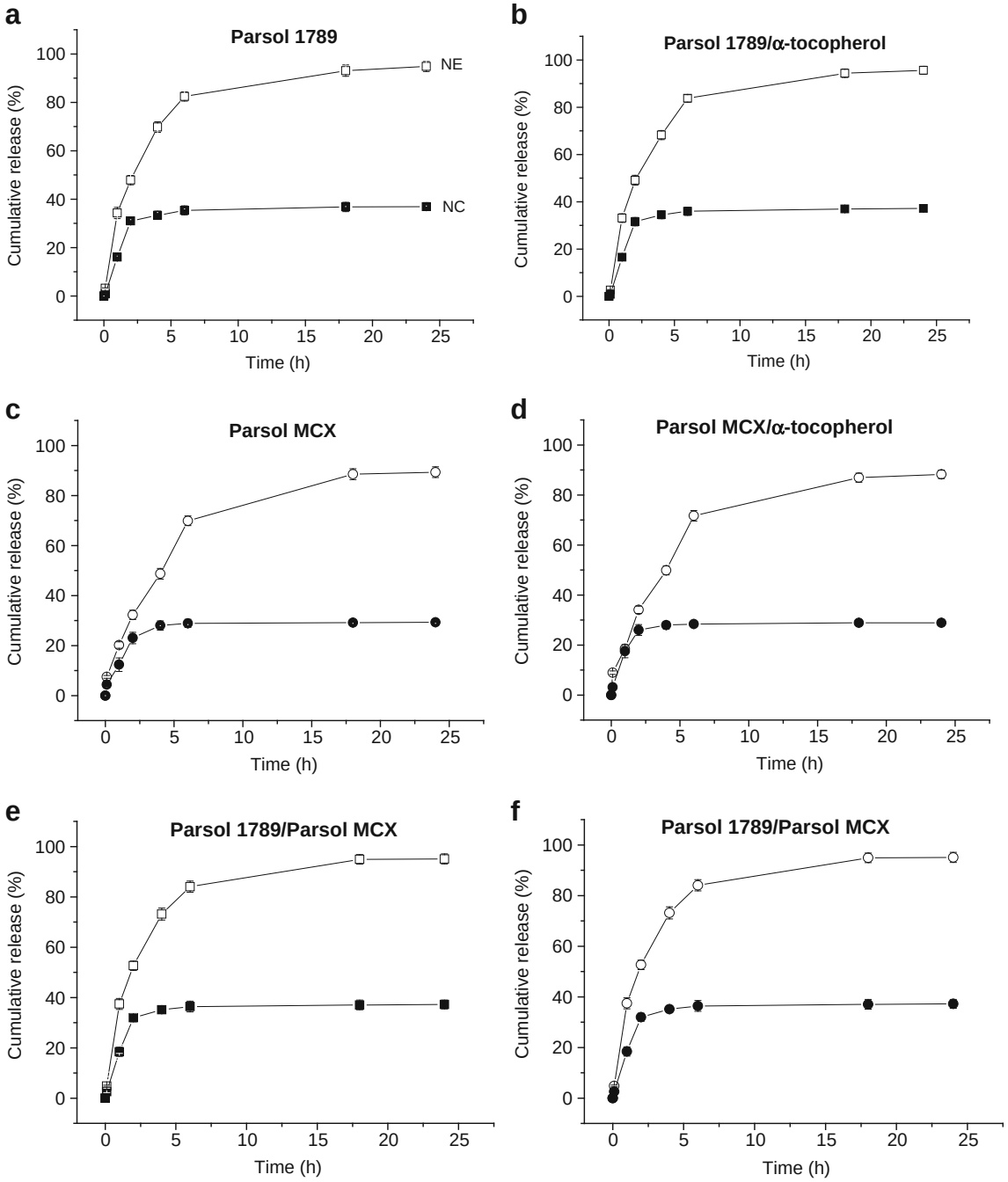

Fig. 6 : *In vitro* cumulative Parsol® 1789 (square symbols) and Parsol® MCX (circle symbols) released from NCs (filled symbols) and NEs (open symbols). Oil phase was composed of Parsol® 1789 (**a**), Parsol® 1789/α-tocopherol (**b**), Parsol® MCX (**c**), Parsol® MCX/α-tocopherol (**d**) and Parsol® 1789/Parsol® MCX (**e** and **f**).

composed of α-tocopherol, the mean hydrodynamic diameters increased from 270 to 298 nm when the oil content was increased from 200 to 400 mg. However, when the oil content was progressively increased from 400 to 600 mg, traces of oil were detected at the surface of the formulations and a second population of large NCs (5 μm) appeared (Table III). Finally, phase separation was observed when the oil content was increased from 600 to 1000 mg (Table III). These results clearly demonstrated that stable NCs obtained by the spontaneous emulsification combined

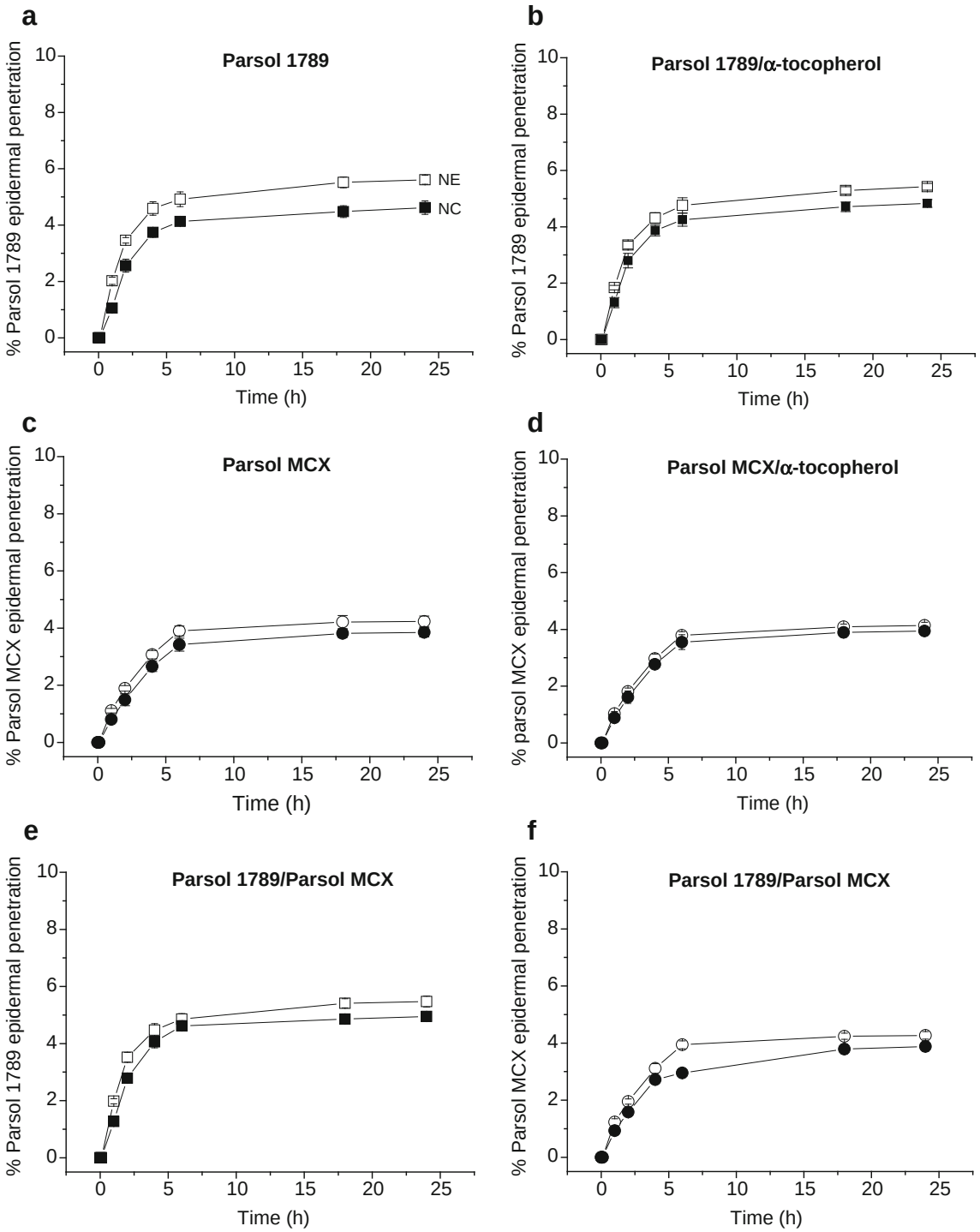

Fig. 7 Epidermal penetration profile of Parsol® 1789 (square symbols) and Parsol® MCX (circle symbols) released from NCs (filled symbols) and NEs (open symbols). Oil phase was composed of Parsol® 1789 (**a**), Parsol® 1789/α-tocopherol (**b**), Parsol® MCX (**c**), Parsol® MCX/α-tocopherol (**d**) and Parsol 1789®/Parsol® MCX (**e** and **f**).

to interfacial polycondensation method occurred only for oil concentration lower than 2% w/v in the organic phase.

In these conditions, whatever oil composition, NEs and NCs were successfully prepared and the mean hydrodynamic diameters were lower than 200 nm and 450 nm respectively (Table IV). The difference between the mean hydrodynamic diameters of the NEs and the NCs, also reported for polyurethane NCs obtained by interfacial polycondensation and spontaneous emulsification (11), was confirmed by SEM and TEM observations. One explanation of this difference comes from the mechanism of the spontaneous emulsification. In the case of NEs, the solvent diffusion results from oil nucleation and growth. However, in the presence of the monomers, the spontaneous emulsification was combined to the interfacial polycondensation resulting in NCs with higher diameters. As these two phenomena are very complex and fast, down to the region of milliseconds (10), only the final states corresponding to the formation of NEs and NCs were observed.

The incorporation of the sunscreen filter in oil-containing polyamide NCs was successful as demonstrated by a total yield of encapsulation higher than 98% of the initial amount of sunscreen used in the preparation (Table V). This gives an idea about the efficacy of polyamide NCs in encapsulating these lipophilic sunscreens. This result is consistent with other studies where high loading efficiencies were obtained upon the encapsulation of lipophilic drugs into NCs. For example, the yield of encapsulation was ~80% for primidone (39), and higher than 90% for indomethacin NCs (40), α-tocopherol NCs (9, 11) or solid lipid nanoparticles (SLN) (41).

Effect of Polymeric Shell on *In Vitro* Sunscreen Release

The release of the sunscreen filters from NEs and NCs was investigated by using a membrane-free model over 24 h. As we can see from Fig. 6, the release of both studied sunscreens from NEs after 24 h was about three times higher than their release from NCs. In the case of NCs of Parsol® MCX, the percentage of released filter after 24 h was (29.27 ± 1.06)% instead of (89.33 ± 2.11)% for NE containing the same sunscreen filter. In the case of NCs containing Parsol® 1789 the percentage of the released filter after 24 h was (36.91 ± 1.67)% instead of (94.83 ± 2.11)% for NE.

Polyamide shell structure allowed to control the release of the encapsulated filter. It has been demonstrated for polyamide microcapsules that the addition of a trifunctional amine such as DETA allowed the control of the mechanical properties, the porosity (42) and the permeability of the microcapsule membrane (43). The release rates from these microcapsule membranes were immeasurably low.

Furthermore, it has been demonstrated by Bouchemal *et al.* (11) that polyamide film is composed of 10% w/w of the polymer and 90% w/w of water. The water contained in the polyamide layer acts like a "physico-chemical obstacle" for the highly lipophilic sunscreen agent diffusion. The swelling of the polymer represents an important parameter allowing to control drug release from microcapsules (44).

Effect of Polymeric Shell on *Ex Vivo* Sunscreen Skin Penetration

In this study, the penetration of both studied sunscreen filters through the epidermis of ear pigs was *ex vivo* investigated during 24 h. As we can see from the results presented in Fig. 7, the lowest percentage of penetration after 24 h was obtained in the case of NCs composed of Parsol® MCX (3.85 ± 0.16)%, while the highest percentage of penetration after 24 h was obtained with of NEs composed of Parsol® 1789 (5.61 ± 0.13)%. Similar results concerning the accumulation of sunscreen filters encapsulated into NCs were obtained by previous researchers. For example, Parsol® MCX NCs composed of poly(ε-caprolactone) were accumulated within the stratum corneum of ear pig skin (7). It was reported in the same work that the use of these NCs did not appear to increase skin permeation.

In all cases, the epidermal penetration is considered to be low for NEs and NCs, while the release values are much higher for NEs (around 95%) than NCs (less than 40%). The high affinity of the lipophilic sunscreen filters towards the stratum corneum can explain their low epidermal penetration even for NEs. The low sunscreen penetration in all cases is a desirable result, since the

Table VI Comparison of SPF Value of NC Preparations with Normal EMs Containing the same Proportion of Sunscreens

Preparation	Mean SPF	Star Category
Parsol® MCX Free EMs	2.93 ± 0.87	No Claim
Parsol® MCX NCs	3.11 ± 0.76	No Claim
Parsol® 1789 Free EMs	1.51 ± 0.48	Ultra
Parsol® 1789 14% *w/w* in Finsolv® TN NCs	1.39 ± 0.41	Ultra
Parsol® 1789 + Parsol® MCX Free EMs	3.86 ± 0.92	Good
Parsol® 1789 25% *w/w* in Parsol® MCX NCs	3.97 ± 0.84	Good

place of the activity of sunscreen filters is in the stratum corneum, so this low penetration ensures that encapsulated sunscreens will not penetrate the dermis and will stay in the epidermis layer, the place of their activity. This property is particularly important for sunscreens because it has been suggested that the amount of sunscreen inside the stratum corneum may be directly related to its SPF value (45).

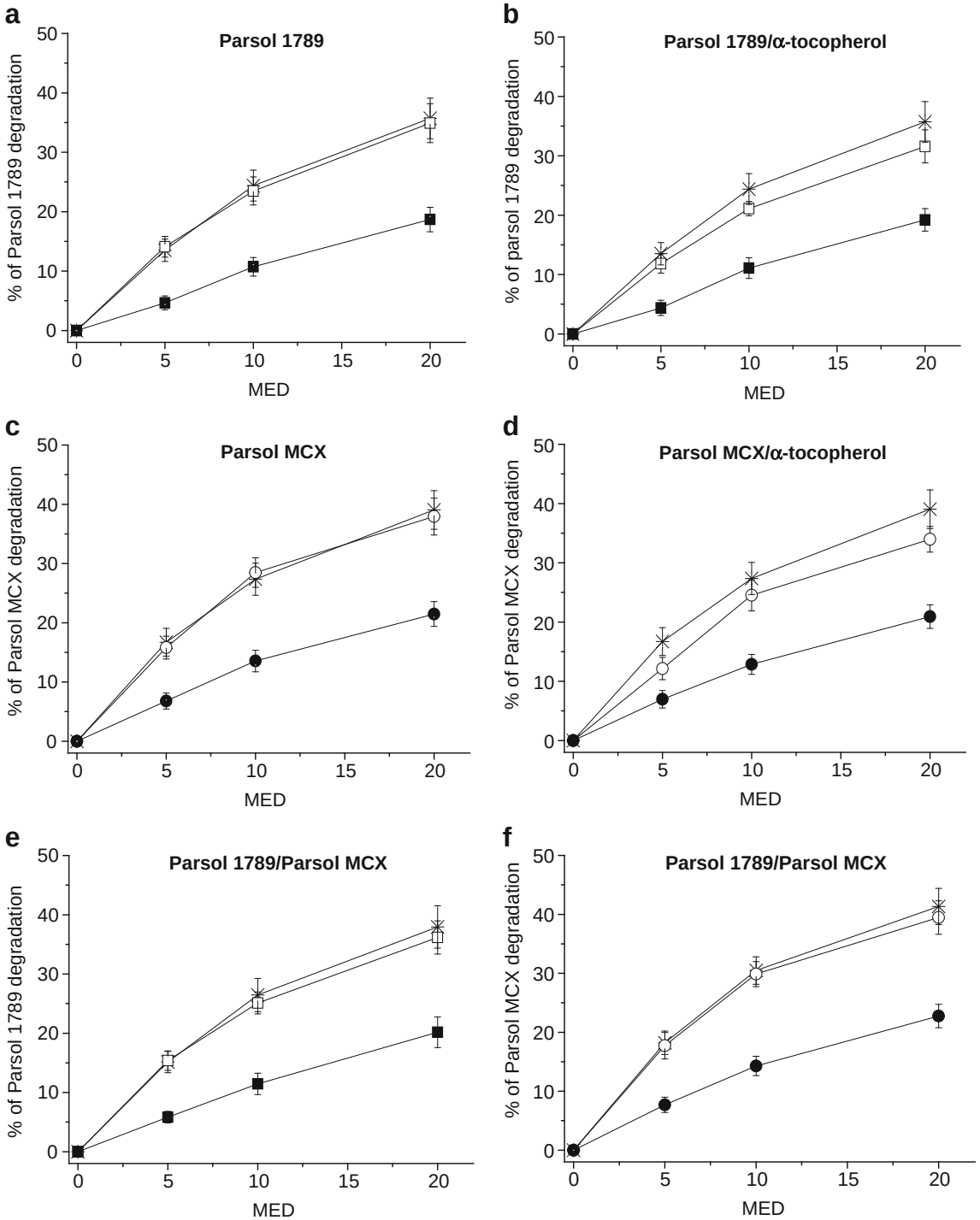

Fig. 8 Comparison of the degradation of Parsol® 1789 (square symbols) and Parsol® MCX (circle symbols) released from emulsions (*), NCs (filled symbols) and NEs (open symbols). Oil phase was composed of Parsol® 1789 (**a**), Parsol® 1789/α-tocopherol (**b**), Parsol® MCX (**c**), Parsol® MCX/α-tocopherol (**d**) and Parsol® 1789/Parsol MCX (**e** and **f**).

Effect of Polymeric Shell on Sunscreen Activity and Photo-stability

The activity of encapsulated sunscreens was verified by comparing the SPF values of NC preparations with emulsions contained the same proportion of free sunscreens. Table VI shows that the two means of SPF for the NCs and the emulsions are not significantly different. We can thus confirm that the activity of the sunscreens encapsulated inside the polyamide NCs did not change their activity.

Photo-stability improvement of encapsulated sunscreens was then verified by comparing the percentage of degradation of encapsulated Parsol® MCX and Parsol® 1789 with NEs and emulsions contained the same proportion of free sunscreens.

All the photo-stability experiments were conducted during 10 min. At this time, no more than 3% of the sunscreen filter was released for both NCs and NEs as indicated in Fig. 6. For Parsol® MCX and Parsol® 1789 encapsulated into NCs, approximately 5–20% of the sunscreen filters were degraded depending on the MED range between 5 and 20 (Fig. 8). This means that the UV rays degraded the free sunscreen released from the NCs (around 3%) but also a part of the encapsulated sunscreen (around 17%). We noted that for both encapsulated sunscreens, either separated or mixed together, their degradation is about 50% lower than that observed as free sunscreens in the case of emulsions or NEs. These results confirmed the ability of the polyamide film to protect the encapsulated Parsols from UV ray degradation.

Effect of α-Tocopherol on Sunscreen Release, Skin Penetration and Photo-stability

Many previous research works demonstrated that α-tocopherol was highly efficient in reducing late radiation-induced skin damage (14–16). Furthermore, α-tocopherol is largely used as supplement for cosmetics to improve sunscreen photo-protection and photo-stability (17). The effect of α-tocopherol addition on sunscreen release, penetration and photo-stability was thus studied for all NC preparations and compared to NEs. As presented in Figs. 6 and 7, the presence of α-tocopherol had no influence on the release rate of the sunscreen filters and on the skin penetration for either NE and NC preparations. Interestingly, the presence of α-tocopherol allowed to improve photo-stability of Parsol® MCX and Parsol® 1789 in the form of NE (Fig. 8). Whatever NE formulation, the percentage of damaged sunscreens in the presence of α-tocopherol was 10% lower than their degradation without α-tocopherol. However, this effect was not remarkable in the case of NCs. This result is due to the encapsulation of sunscreens inside the polyamide polymer which improved significantly their photo-stability of about 50% in comparison with NEs. Consequently, their degradation was already low and it was not possible to remark the effect of α-tocopherol on their photo-stability.

CONCLUSION

NEs and polyamide NCs, as carrier for sunscreen filters, were successfully prepared with suitable mean size and yield of encapsulation. The encapsulation of Parsol® MCX and Parsol® 1789 into polyamide NCs ensured their controlled release in comparison with NEs. Interestingly, sunscreen skin penetrations through the epidermis for NEs and NCs were very low. This result warrantee that sunscreens, will stay in the stratum corneum, the site of their activity. The activity of encapsulated Parsol® MCX and Parsol® 1789 did not change, in comparison with the activity of the same not encapsulated sunscreens. Photo-stability of encapsulated sunscreens in NCs form increased about 50%, compared with the photo-stability of the same not encapsulated sunscreens, while NEs form did not influence the photo-stability of sunscreens. The presence of α-tocopherol increased the photo-stability of sunscreens in the form of NEs. However, this effect was not remarkable in the case of NCs.

ACKNOWLEDGMENTS & DISCLOSURES

Nicolas Tsapis, Mounia Makhoukh, Ludivine Houel were gratefully thanked for their help for microscopic observations. Claire Troufflard and France Costa-Torro were gratefully thanked for their help for NMR analyses.

REFERENCES

1. Trenti R (2007) Prodotti funzionali: Fotostabilità dei filtri solari, Manuale del cosmetologo, Ed. Tecniche Nuove, Milano, 406–407
2. Trenti R (2007) Prodotti funzionali: Prodotti solari e dopo sole, Manuale del cosmetologo, Ed. Tecniche Nuove, Milano, 402–407
3. Proserpio G (1985) Radiazioni e loro azione sulla cute: Abbronzatura, Filtri UVB—UNA, Fattori di pigmentazione, Chimica e tecnica cosmetica, Ed. Sinerga, Pero—Milano, 406–422
4. Wang SQ, Balagula Y, Osterwalder U. Photoprotection: a review of the current and future technologies. Dermatologic Therapy. 2010;23:31–47.
5. Pfluecker F, Driller HJ, Vouzellaud L, Marchio F, Guinard H, Chaudhuri R. Encapsulated sunscreen composition that does not penetrate skin, World Intellectual Property Organization patent. WO. 2003;2003011239:A2.
6. Alvarez-Roman R, Barré G, Guy RH, Fessi H. Biodegradable polymer nanocapsules containing a sunscreen agent: preparation and photoprotection. Eur J Pharm Biopharm. 2001;52:191–5.

7. Alvarez-Roman R, Kail A, Kalia YN, Guy R, Fessi H. Enhancement of topical delivery from biodegradable nanoparticles. Pharm Res. 2004;21(10):1818–25.
8. Chaudhuri RK (2007) Photostable organic sunscreen composition, US Patent 7166273
9. Bouchemal K, Briançon S, Perrier E, Fessi H, Bonnet I, Zydowicz N. Synthesis and characterization of polyurethane and poly(ether urethane) nano-capsules using a new technique of interfacial polycondensation combined to spontaneous emulsification. Int J Pharm. 2004;269(1):89–100.
10. Bouchemal K, Couenne F, Briançon S, Fessi H, Tayakout M. Polyamides nanocapsules: modelling and wall thickness estimation. AIChE J. 2006;52(6):1–10.
11. Bouchemal K, Couenne F, Briançon S, Fessi H, Tayakout M. Stability studies on colloidal suspensions of Polyurethane nanocapsules. J Nanosci Nanotechno. 2006;6:9–10.
12. Bouchemal K, Briançon S, Fessi H, Chevalier Y, Bonnet I, Perrier E. Simultaneous emulsification and interfacial polycondensation for the preparation of colloidal suspension of nanocapsules. Mat Sci Eng C. 2006;26:472–80.
13. Vauthier C, Bouchemal K. Methods for the preparation and manufacture of polymeric nanoparticles. Pharm Res. 2009;26 (5):1025–58.
14. Laurent C, Pouget J-P, Voisin P. Modulation of DNA damage by pentoxigylline and α-tocopherol in skin fibroblasts exposed to gamma rays. Radiation Res. 2005;164:63–72.
15. Wu S, Gao J, Dinh QT, Chen C, Fimmel S. IL-8 production and AP-1 transactivation induced by UVA in human keratinocytes: roles of D-alpha-tocopherol. Mol Immunol. 2008;45:2288–96.
16. Masaki H. Role of antioxidants in the skin: Anti-aging effects. J Dermatol Sci. 2010;58:85–90.
17. Wu Y, Matsui MS, Chen JZS, Jin X, Shu C-M, Jin G-Y, *et al.* Antioxidants add protection to a broad-spectrum sunscreen. Clin Exp Dermatol. 2010;36:178–87.
18. Bouchemal K, Briançon S, Perrier E, Fessi H. Nano-emulsion formulation using spontaneous emulsification: solvent, oil and surfactant optimization. Int J Pharm. 2004;280(1–2):241–51.
19. Bouchemal K, Briançon S, Chaumont P, Fessi H, Zydowicz N. Microencapsulation of Dehydroepiandrosterone (DHEA) with poly (ortho esters) polymers by interfacial polycondensation. J Microencapsul. 2003;20(5):635–51.
20. Bouchemal K, Ponchel G, Mazzaferro S, Campos-Requena V-H, Gueutin C, Palmieri G-F, *et al.* A new approach to determine loading efficiency of Leu-enkephalin in poly(isobutylcyanoacrylate) nanoparticles coated with thiolated chitosan. J Drug Del Sci Tech. 2008;18(6):392–7.
21. Wissing SA, Müller RH. Solid lipid nanoparticles as carrier for sunscreens: *in vitro* release and *in vivo* skin penetration. J Control Release. 2002;81(3):225–33.
22. Dick IP, Scott RC. Pig ear skin as an *in-vitro* model for human skin permeability. J Pharm Pharmacol. 1992;44(8):640–5.
23. Kligman AM, Christophers E. Preparation of isolated sheets of human stratum corneum, *Arch.* Dermatol. 1963;88:702–5.
24. Puglia C, Blasi P, Rizza L, Schoubben A, Bonina F, Rossi C, *et al.* Lipid nanoparticles for prolonged topical delivery: An *in vitro* and *in vivo* investigation. Int J Pharm. 2008;357:295–304.
25. Swarbrick J, Lee G, Brom J. Drug permeation through human skin. I. Effects of storage conditions of skin. J Invest Dermatol. 1982;78:63–6.
26. Matts PJ, Alard V, Brown MW, Ferrero L, Gers-Barlag H, Issachar I, *et al.* The COLIPA *in vitro* UVA method: a standard and reproducible measure of sunscreen UVA protection. Int J Cosmet Sci. 2010;32:35–46.
27. Diffey BL, Robson J. A new substrate to measure sunscreen protection factors throughout the ultraviolet spectrum. J Soc Cosmet Chem. 1989;40:127–33.
28. Berset G, Gozenbach H, Christ R, Martin R, Deflandre A, Mascotto RE, *et al.* Proposed protocol for determination of photostability. Part I: cosmetic UV filters. Int J Cosmet Sci. 1996;18:167–77.
29. Davis RD, Steadman SJ, Jarrett WL, Mathias LJ. Solution ^{13}C NMR characterization of nylon 66: quantification of cis amide conformers, acid and amine end groups. Macromolecules. 2000;33:7088–92.
30. Lauprêtre F, Eustache R-P, Monnerie L. High-resolution solid-state ^{13}C nuclear magnetic resonance investigation of local motions in model epoxy resins. Polymer. 1995;36:267–74.
31. Skrovanek DJ, Howes SE, Painter PC, Coleman MM. Hydrogen bonding in polyamides. Macromolecules. 1985;18:1676–83.
32. Schroeer LR, Cooper SL. Hydrogen bonding in polyamides. J Appl Phys. 1976;47:4310–7.
33. Arimoto H. α–γ Transition of nylon 6. J Polym Sci, Part A: Polym Chem. 1964;2:2283–95.
34. Trifan DS, Terenzi JF. Extents of hydrogen bonding in polyamides and polyurethanes. J Polym Sci. 1958;28:443.
35. Okada A, Kawasumi M, Tajima I, Kurauchi T, Kamigaito O. A solid state NMR study on crystalline forms of nylon 6. J Appl Polym Sci. 1989;37(5):1363–71.
36. Illers KH, Haberkorn H, Lanbo JB. J Macromol Sci Phys B. 1972;6:129.
37. Murthy NS. Metastable crystalline phases in nylon 6. Polym Commun. 1991;32:301–5.
38. Moore WH, Krimm S. Vibrational analysis of peptides, polypeptides, and proteins. I Polyglycine I Biopolymers. 1976;15:2439–64.
39. Ferranti V, Marchais H, Chabenat C, Orecchioni AM, Lafont O. Primidone-loaded poly-varε-caprolactone nanocapsules: incorporation efficiency and *in vitro* release profiles. Int J Pharm. 1999;193:107–11.
40. Calvo P, Vila-Jato JL, Alonso MJ. Comparative *in vitro* evaluation of several colloidal systems, nanoparticles, nanocapsules, and nanoemulsions, as ocular drug carriers. J Pharm Sci. 1996;85:530–6.
41. Müller RH, Mäder K, Gohla S. Solid lipid nanoparticles (SLN) for controlled drug delivery—a review of the state of the art. Eur J Pharm Biopharm. 2000;50:161–78.
42. Mathiowitz E, Cohen MD. Polyamide microcapsules for controlled release. I Characterization of the membranes. J Membrane Sci. 1989;40:1–26.
43. Janssen LJJM, Boersma A, te Nijenhuis K. Encapsulation by interfacial polycondensation. III. Microencapsulation; the influence of process conditions on wall permeability. J Membrane Sci. 1993;79:11–26.
44. Mathiowitz E, Cohen MD. Polyamide microcapsules for controlled release. I V. Effects of swelling. J Membrane Sci. 1989;40:55–65.
45. Benech-Kieffer F, Wegrich P, Schwarzenbach R, Klecak G, Weber T, Leclaire J, *et al.* Percutaneous absorption of sunscreens *in vitro*: interspecies comparison, skin models and reproducibility aspects. Skin Pharmacol Appl Skin Physiol. 2000;13:324–35.